

Transmission Power Levels Prediction for Distributed Topology Control Protocols within Parameterized Scenarios

Sergio Kostin*, Leonardo Bidese de Pinho and Claudio Luis de Amorim
Parallel Computing Lab – COPPE Systems Engineering Program
Federal University of Rio de Janeiro
Rio de Janeiro, RJ, Brazil 21941–972, PO BOX 68.511
Email: {kostin,leopinho,amorim}@cos.ufrj.br

Abstract—Distributed Topology Control Protocols (DTCP) for Wireless Sensor Networks (WSN) coordinate nodes’ decisions regarding their transmission ranges, in order to set up a network with a certain connectivity, while reducing nodes’ energy consumption and/or increasing network capacity. The key issue in DTCP is to choose the most suitable Transmission Power Level (TPL) among those available for each sensor node in a distributed manner. We present a method to predict the TPL for DTCP in specific realistic scenarios, which takes into account several propagation phenomena, such as barriers and multipath interference. To evaluate the effectiveness of our approach, we simulated the radio propagation pattern of a WSN in a scenario of multiple rooms. Our results suggested that our method allows to predict, with reasonable accuracy, the approximate TPL distribution achieved by different DTCP approaches within a given parameterized scenario.

Index Terms—Wireless; Sensor Networks; Topology; Simulation

I. INTRODUCTION

Over the last years, Wireless Sensor Networks (WSN) have established new information collection and broadcast models, with a great potential for new applications such as environmental monitoring and “intelligent” buildings, just to name a few.

Nevertheless, a major hurdle in deploying a WSN is the limited battery’s life of sensor nodes. As a result, the Transmission Power Level (TPL) often is the key factor affecting the energy consumption, once that the nodes usually consume the same power when they are in the receiving mode. Thus, estimating suitable TPLs can help strongly the resource management, by determining, for example, when the sensor node’ battery will probably become flat.

In this work, we present a method that can predict TPLs for Distributed Topology Control Protocols (DTCPs) in scenarios with obstacles. Specifically, our

method calculate the discrete TPL that should be used given a certain deployment area of WSN with its configuration of obstacles and a probabilistic distribution of sensor nodes.

Our method is based on two metrics we recently proposed [1]: the Blockage Rate (BR) and the Useful Area Rate (UR). Roughly, BR accounts for the interaction between transmitters and receivers considering multipath interference and signal sensitivity due to the presence of obstacles for a given probabilistic distribution of receiver positions in the scenario. UR concerns with the loss effects in a given propagation path. More specifically, the two metrics take into account the average values of the radiation parameters, including the rate of electromagnetic emission blockage, the radiation rate outwards the scenario, the effect of multipath interference, and the percentage of radiation effectively used. We use a combination of the two metrics to estimate the connectivity as function of TPL.

To assess the effectiveness of our approach, we simulated the deployment of a WSN in an indoor scenario of multiple offices. Our results showed that our method allows to estimate, with reasonable accuracy, the TPL distribution that will be chosen by DTCPs for a specific scenario. In summary, the main contributions of this work are: *i*) a probabilistic spatial model regarding connectivity aspects considering electromagnetic phenomena; and *ii*) a method of estimating the TPL for DTCPs in such environments.

The remainder of the paper is organized as follows. Section II overviews briefly the basic Topology Control theory and presents related work. In section III, we introduce our technique for establishing the transmission power levels in WSNs for a given scenario. Section IV describes our experimental method and analyzes simulated results. Finally, our conclusion and ongoing works are presented in Section V.

*Corresponding author. Also affiliated to the Military Institute of Engineering – Praca Gen Tiburcio, 80 – Rio de Janeiro, RJ, Brazil
Email: kostin@ime.eb.br

II. BRIEF OVERVIEW ON TOPOLOGY CONTROL THEORY AND RELATED WORK

The simplest software approach for radio-wave propagation modeling at high frequencies (VHF to SHF) is semi-empirical, such as the well-known exponential path-loss model. Radiowave propagation models using detailed terrain databases are commonly referred as Site Specific Propagation models (SISP) [2]. Smaller scenarios (usually indoors) may benefit from more complex and accurate approaches such as ray-tracing modeling. In this technique, the main propagation paths (rays) are deterministically found based on the common electromagnetic phenomena of reflection, refraction, and scattering, which includes diffraction. Ray-tracing is usually carried out two-fold, using either greedy methods or image theory [3]. With the ever growing available numerical capacity of computers, ray-tracing models have increasingly become more attractive as propagation prediction tools. Some researchers even expect that deterministic modeling may prevail in a near future, as the preferred approach for propagation prediction, even outdoors [2].

Topology Control (TC) is the art of coordinating nodes' decisions regarding their transmission ranges, in order to generate a network with the desired properties (e.g. connectivity) while reducing node energy consumption and/or increasing network capacity [4]. A topology control protocol should have some basic properties: be fully distributed and asynchronous; be localized; generate a topology that preserves the original network connectivity and relies, if possible, on bidirectional links; generate a topology with small physical degree; and rely on 'low-quality' information [4]. Usually, Distributed Topology Control Protocols (DTCPs) solutions use a bottom-up approach, such as CTBC [5] and KNEIGHLEV [6] in which the sensor nodes start either from a lower transmission power level (TPL) up to a higher suitable TPL that often is more economic but takes longer to converge, or the transmitters start with higher TPLs (K-NEIGH [7], LSP [8] and XTC [9] stepping down to a suitable TPL, thus spending more power though converging faster.

However, often the TPL of a node cannot be set to an arbitrary level. Instead, the transmitters can only be set to a limited number of predefined power levels. DTCPs that fit in this category are called Level-Based Topology Control Protocols (LBTCP) [4]. Among several solutions of LBTCP we can cite COMPOW [10], CLUSTERPOW [11] and KNEIGHLEV [6].

The present work presents a novel way to predict the TPLs for LBTCP within a parameterized scenario.

III. TRANSMISSION POWER CONTROL TECHNIQUE

Our technique is based on two metrics: Blockage Rate (BR) and Useful Area Rate (UR) [1].

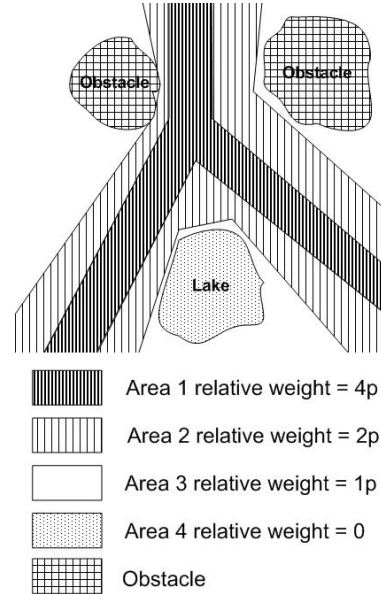


Fig. 1. Probabilistic Spatial Distribution Map (PSDM)

A. Occupation Profile of a Scenario

BR and UR are calculated for each particular scenario. Often, we can use a Geographic Information System (GIS) to build a Probabilistic Spatial Distribution Map (PSDM). The idea behind PSDM is that distributed sensor nodes within a WSN scenario tend to form specific probabilistic occupation profiles. For example, pedestrians usually walk along sidewalks, gardens and parks. Cars are driven on roads, avenues and so on. Therefore, it is always possible to derive the PSDM using the location of the sensor nodes distributed in a specific scenario, mobility models [12], or calculated by means of a localization system [13] which indicates the probable region where each sensor is located.

Figure 1 shows an example of a receiver device's PSDM based on the relative weights of the distributed occupation across the terrain by the transceivers. These weights are obtained from a given probability density. The distribution can be function of time and number of transceivers. It can also be conditional ($P(A | B)$). Specifically, in Figure 1 the area with $p = 4, 3, 2, 1$ represent streets, sidewalks, gardens, and a lake, respectively.

B. Blockage Rate (BR)

Figure 2 shows a typical situation where a certain obstacle blocks the electromagnetic signal of a transmitter t , establishing four distinct areas regarding the quality of signal reception: the receivers' area (RA) - e.g. the area where the receivers are located, the theoretical coverage area not contained in RA, the coverage area contained in RA blocked by the obstacles (E_B), and the

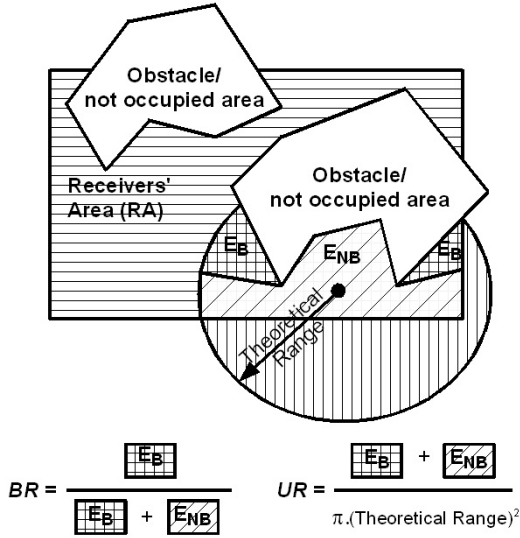


Fig. 2. Blockage Rate and Useful Area Rate

area unblocked (E_{NB}). Conceptually, BR expresses the ratio between E_B and the sum given by $E_B + E_{NB}$.

Formally, considering a specific transmitter class located at position s , and assuming a specific transmission power level pw , then $BR(t(s, pw))$ is defined by:

$$\frac{\sum_{x \in RA} P(r_j(x) | t(s)) B_{CF}(t(s, pw), r_j(x))}{\sum_{x \in RA} P(r_j(x) | t(s)) B_{NF}(t(s, pw), r_j(x))} \quad (1)$$

In Equation 1, $P(r_j(x) | t(s))$ represents the probability that the j^{th} receiver, r_j , be found at x position, subjected to a t -type transmitter being located at position s . Note that the expression accommodates clustering (when devices tend to join) and repelling (when there is a minimum distance among devices). The antenna gains of transmitters and receivers are considered in the calculation of the probabilities, as well as the receivers' sensitivities. The Function B accounts for the interaction between transmitters - $t(s, pw)$ (transmitter t at s , emitting a signal with pw power level) - and receivers - (receiver r_j) - within RA. The subscripts CF and NF mean *Considering Fading* and *Not considering Fading*, respectively.

$B_{CF} \in \{-1, 0, 1\}$. B_{CF} returns 0 when the receiver $r_j(x)$ is in the theoretical coverage area of a transmitter t at a pw power level, the received signal is above the data sensitivity level and the multipath interference is so weak that it is unable to degrade the data link (a power level threshold must be established to assist this process). Otherwise B_{CF} returns 1, either when the degradation due to multipath is observed or the received signal is below the data sensitivity level. B_{CF} will return

-1 when the receiver is outside the theoretical coverage area, since multipath interference may also cause a constructive effect (at aisles, for example), though the obstacle configuration is such that the transmitted signal is still able to reach the receiver r_j .

$B_{NF} \in \{0, 1\}$. B_{NF} simply considers free-space propagation and the presence of obstacles against direct rays. It returns 1 for all receivers $r_j(x)$ within the theoretical coverage area of the transmitter t at position $s - t(s, pw)$. Otherwise B_{NF} equals zero, i.e., when the receiver r_j is at a position x such that it is either outside (beyond) the theoretical coverage area of t , or behind any obstacle (no direct ray reaches the receiver).

We calculate BR for a specific Transmitter Area (TA), computing the weighted average of all $BR(t(s, pw))$ according to Equation 2. Other statistical parameters such as standard deviation, median, maximum, minimum, etc., are also calculated in order to provide the best possible description of the chosen scenario. We may also compute the first and the second derivatives with respect to TPL (pw) to help with the analysis on overcoming propagation barriers.

$$BR(TA, t, pw) = \frac{\sum_{s \in TA} P(t(s)) BR(t(s, pw))}{\sum_{s \in TA} P(t(s))} \quad (2)$$

C. Useful Area Rate (UR)

Figure 2 illustrates the notion of Useful Area Rate (UR) that expresses the ratio between the useful and the theoretical coverage area of a transmitter node. The definition of useful coverage area comprises the theoretical coverage area of a transmitter that lies within the receiver area ignoring the obstacles. Therefore, this metric is most concerned with free-space coverage and aspects of signal range in the WSN, thus ignoring multipath effects and scattering. Formally, given a certain transmitter class t , located at s , operating at a power level pw , $UR(t(s, pw))$ is defined by:

$$\frac{\sum_{x \in RA} U_{CO}(t(s, pw), r_j(x))}{\sum_{x \in \text{Theoretical Range}} U_{NO}(t(s, pw), r_j(x))} \quad (3)$$

In Equation 3, Function U verifies the interaction between the theoretical coverage area and the scenario's obstacles. The subscripts CO and NO mean *Considering Obstacles* and *Not Considering Obstacles*, respectively.

$U_{CO} \in \{0, 1\}$. Function U_{CO} returns 1 when the receiver r_j is in the theoretical coverage area, or in RA, either in a position where $P(r_j(x) | t(s))$ is not equal to 0. Otherwise, it returns 0.

$U_{NO} \in \{0, 1\}$. U_{NO} quantifies the coverage area, considering r_j 's sensitivity. UR mainly aims at the loss

effects of propagation paths, neglecting the probabilistic distribution of receiver's position that has already been considered in BR .

D. How to Determine the Connectivity Using BR and UR

Consider $CA(t(s, pw), r_j)$ as the theoretical coverage area of a transmitter t operating at a power level pw for a specific receiver r_j . Yet, consider D as the sensor node density and $t(s, pw) = z$. When we carry out the product:

$$C(z) = (1 - BR(z))UR(z)CA(z, r_j)D \quad (4)$$

We will get a specific connectivity for that position. We can expand Equation 4 to a region, as we made to $BR(TA, t(pw))$, and calculate various statistical moments. The mean, for example, is given by Equation 5.

$$C(TA, t(pw), D) = \frac{\sum_{s \in TA} P(t(s))C(t(s, pw), D)}{\sum_{s \in TA} P(t(s))} \quad (5)$$

E. Predicting the TPL Distribution

Using this information obtained in the previous subsection, we can predict the TPL distribution in the network, specially in protocols that intend to conserve energy, such as XTC, KNEIGH and KNEIGHLEV.

The way to calculate the distribution is straight forward, according to Equation 6.

$$Dist(TA, k, pw_i) = P(TA, k, pw_i) - P(TA, k, pw_{i-1}) \quad (6)$$

$Dist(TA, pw_i)$ means the percent of the transmitters inside a TA, which wants to connect to k nodes using the TPL of pw_i . $P(TA, k, pw_i)$ is the probability of a sensor s be connected to k neighbors transmitting at power level pw_i .

IV. SIMULATION

In this section, we evaluate the benefits that BR and UR metrics can offer to establish the TPL scheme for a WSN. Specifically, we simulated the deployment of a WSN in a scenario of multiple offices, for which we computed BR , UR , and C , and then used these results to determine the most efficient transmission power levels for the sensor nodes of the WSN for each scenario room.

A. The Zerkalo Simulator and Simulation Parameters

We developed a simple SISP tool called *Zerkalo* (*mirror* in Russian) based on ray-tracing (images method) [3] that simulates the electromagnetic propagation in a given scenario. Besides free-space propagation, *Zerkalo* also simulates the electromagnetic phenomena of reflection

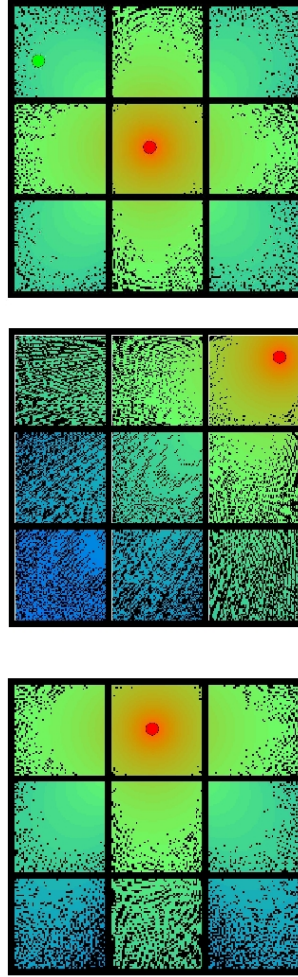


Fig. 3. Radiation pattern of sensors in each scenario room

and refraction by computing the multipath interference due to reflections up to a desired order. *Zerkalo*'s algorithm complexity is $O(n^r)$, where r is the reflection order and n is the number of obstacles.

In the design of *Zerkalo*, we assumed the so-called *narrowband* hypothesis considering that the transmitted signal's spectral content is narrow enough around the carrier (dozens or hundreds of KHz depending on the conditions) so that the technique fading can be considered flat [2]. The points most affected by this kind of fading are those close to walls, specially the ones near the corners [14].

B. Test Scenario

The test scenario, shown in Figure 3, is composed of 9 rooms ($15 \times 15 \text{ m}^2$ each), similarly arranged as in the tic-tac-toe game. The rooms are apart by 15 cm wide brick walls with relative permittivity (ϵ_r) equal to 4.444.

We computed the metrics as defined in Section 3 for transmitters at CENTRAL, CORNER, and LATERAL

rooms, considering up to second order reflections ([15] shows that only the first reflection has significant power under most situation). Moreover, we have also assumed the following test parameters: 0.122 m wavelength, receiver sensitivity is -70 dBm (receive threshold), -85 dBm (carrier sense threshold), half wave dipole antennas (1.64 dB gain) for transmission and reception [2], the capture threshold is 10 dB, and the MAC is based on CSMA/CA. We have modeled the error in the RSSI as 10% of receive power around the correct value. In the present test scenario, the antennas' heights were half way between floor and roof, such that the major propagation effects were concentrated on the horizontal plane comprising all antennas, simplifying the propagation problem to a 2D analysis.

Regarding the influence of interference, the BR metric uses a threshold value that defines whether or not to consider a resulting fading. For the analysis presented below, we assumed a threshold value of half the power received in the main propagation path that is usually the direct path. Specifically, if the (complex) sum of all the multipath phasors is below half of the main component power, then $B_{CF} = 0$. Otherwise, B_{CF} returns 1 or -1 , for destructive or constructive interference, respectively. Figure 3 illustrates how *Zerkalo* computes path loss, with multipath interference and the radiation in the three rooms located at the center, the corner, and the lateral, respectively. The darkest points in Figure 3 show the most affected points by the multipath interference, considering the transmitter relative position. We assume that the nodes are placed uniformly at random in the scenario with density occupation of all rooms as being 0.05 sensors by square meter.

C. Connectivity Aspects

We solved the Equation 4 with the above criteria for assessing the WSN connectivity. As a result, a table was built and stored in the sensor node with the following statistical parameters, specially the cumulative distribution. The summarized results are represented as a graphic as shown in Figure 4.

Let us assume that a given sensor node located in the CENTER ROOM should be interconnected to other 40 sensor nodes. According to our technique, this sensor node will look up its table checking on possible values that allow it to achieve that connectivity degree. As can be seen in Figure 4, only TPLs set at least to 2 dBm will attend the required connectivity with probability greater than zero. If 6 dBm is chosen, there is a probability about 50% of reaching 40 nodes. For 8 dBm, the chance is greater than 75%. Finally, from 10 dBm upwards the connectivity degree of 40 nodes is almost always reached. However, outliers events can happen. For example, connectivity degree (k) greater than 40 with TPL

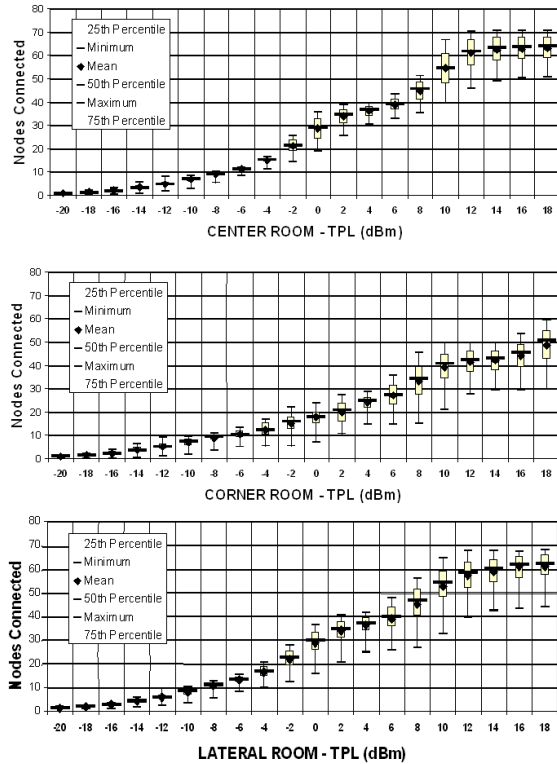


Fig. 4. Connectivity x TPL

smaller than 2 dBm and $k < 40$ with TPL greater than 10 dBm.

D. Prediction Results and Analysis

Considering that the LATERAL ROOMS and the CORNER ROOMS represent 89% (8/9) of the scenario area, we concentrated our analysis on those areas. As comparison, we use the KNEIGHLEV [6] protocol and a level-based *one-hop* implementation of XTC [9], without the step of edge selection (regarding the *two-hop* optimization). In such a case, XTC preserves network connectivity in the worst case, while KNEIGHLEV gives only a probabilistic guarantee on network connectivity. We conducted 30 random simulations for each DTCP according to the parameters of subsection IV-B.

The results are shown in Tables I and II. The first column (TPL) represents the TPL (in dBm). The second column (P(ROOM)) shows the cumulative percentage probability of reaching a certain connectivity degree according to our method. The third column (D(ROOM)) represents the computed value of Equation 6. Fourth and Fifth columns show the TPL distribution of XTC and KNEIGHLEV. Note that the sum of the third, fourth, and fifth columns are less or equal to 100.

The optimization of the *two-hop* links achieved energy savings. In both cases – CORNER (CR) and LATERAL

TABLE I
LATERAL ROOM TPL DISTRIBUTION FOR $k=40$

TPL	P(LR)	D(LR)	D(XTC)	D(KNEIGHLEV)
0	-	-	-	2
2	2	2	4	22
4	14	12	9	48
6	47	33	2	23
8	73	26	3	5
10	91	18	18	-
12	99	8	26	-
14	100	1	21	-
16	100	-	9	-
18	100	-	5	-
>18	100	-	3	-

TABLE II
CORNER ROOM TPL DISTRIBUTION FOR $k=40$

TPL	P(CR)	D(CR)	D(XTC)	D(KNEIGHLEV)
0	-	-	-	-
2	-	-	-	-
4	-	-	-	-
6	-	-	-	-
8	9	9	-	10
10	25	16	7	22
12	35	10	28	36
14	40	5	18	24
16	55	15	8	6
18	75	20	12	2
>18	100	25	27	0

(LR) rooms – our estimates fit between both distributions. The outside results from *one-hop* implementation of XTC (related to the worst cases) are upper bounds for our estimates and the *two-hop* optimization of KNEIGHLEV induces a result that is a lower bound for our estimation.

It is worth to note that the proposed method allows the construction of protocols based on TPL planning instead of using feedback mechanisms. It would be particularly useful in mobile environments, specially because, as stated in [4], mobile DTCP must be fast to build the topology, so that it can catch up with the changes that happen across the network. To be fast, a protocol should exchange relatively few messages with neighboring nodes and should execute a simple algorithm to compute the neighboring set. Both characteristics are provided by our method.

V. CONCLUSION

This work has proposed a novel method for TPLs distribution prediction for WSN in scenarios with obstacles. Our method is supported by two metrics, the Blockage Rate (BR) and the Useful Area Rate (UR) – that are able to correlate WSN connectivity degree with distributed sensor TPLs under the effects of propagation barriers and multipath fading.

To evaluate the potential of our technique, we simulated in detail the electromagnetic propagation of a

WSN test scenario of multiple rooms with obstacles. The simulated results showed that the method could estimate with reasonable accuracy the TPL distribution in such an environment.

As further works, we plan to extend our technique to work in mobile networks, in 3D scenarios, with different antenna heights, and to aggregate other radio irregularities besides multipath interference.

REFERENCES

- [1] S. Kostin and C. L. de Amorim, "Transmission Power Control for Wireless Sensor Networks in Scenarios with Obstacles," in *Proceedings of the 25th Brazilian Symposium on Computer Networks (SBRC)*, vol. 1, Belem, PA, Brazil, May-June 2007, pp. 337–350. (in Portuguese).
- [2] T. S. Rappaport, *Wireless Communication: Principles and Practice*, 2nd ed. Prentice Hall, 2002.
- [3] T. Sarkar, Z. Ji, K. Kim, A. Medouri, and M. Salazar-Palma, "A Survey of Various Propagation Models for Mobile Communication," *IEEE Antennas and Propagation Magazine*, vol. 45, no. 1, pp. 51–82, June 2003.
- [4] P. Santi, *Topology Control in Wireless Ad Hoc and Sensor Networks*, 1st ed. Wiley, September 2005.
- [5] L. Li, J. Y. Halpern, P. Bahl, Y.-M. Wang, and R. Wattenhofer, "A Cone-Based Distributed Topology-Control Algorithm for Wireless Multi-Hop Networks," *IEEE/ACM Trans. Netw.*, vol. 13, no. 1, pp. 147–159, February 2005.
- [6] D. Blough, C. Harvest, G. Resta, G. Riley, and G. P. Santi, "A Simulation-Based Study on the Throughput Capacity of Topology Control in CSMA/CA Networks," in *Proceedings of the Fourth Annual IEEE International Conference on Pervasive Computing and Communications Workshops (PerCom Workshops)*. Pisa, Italy: IEEE Computer Society, March 2006, pp. 13–17.
- [7] D. Blough, M. Leoncini, G. Resta, and P. Santi, "The Lit K-Neigh Protocol for Symmetric Topology Control in Ad Hoc Networks," in *Proceedings of the 4th ACM International Symposium on Mobile Ad Hoc Networking and Computing (MobiHoc)*, Annapolis, Maryland, USA, October 2003, pp. 141–152.
- [8] Y. Shen, Y. Cai, and X. Xu, "A Shortest-Path-Based Topology Control Algorithm in Wireless Multihop Networks," *SIGCOMM Comput. Commun. Rev.*, vol. 37, no. 5, pp. 29–38, October 2007.
- [9] R. Wattenhofer and A. Zollinger, "XTC: A Practical Topology Control Algorithm for Ad-Hoc Networks," in *Proceedings of 4th International Workshop on Algorithms for Wireless, Mobile, Ad Hoc and Sensor Networks (WMAN)*, Santa Fe, New Mexico, USA, April 2004.
- [10] S. Narayanaswamy, V. Kawadia, R. Sreenivas, and P. Kumar, "Power Control in Ad-Hoc networks: Theory, Architecture, Algorithm and Implementation of the COMPOW Protocol," in *Proceedings of European Wireless Conference (EW)*, Florence, Italy, February 2002, pp. 156–162.
- [11] V. Kawadia and P. Kumar, "Principles and Protocols for Power Control in Wireless Ad Hoc Networks," *IEEE Journal on Wireless Ad Hoc Networks*, vol. 23, no. 1, pp. 76–86, January 2005.
- [12] T. Camp, J. Boleng, and V. Davies, "A Survey of Mobility Models for Ad Hoc Network Research," *Wireless Communications and Mobile Computing*, vol. 2, no. 5, pp. 483–502, September 2002.
- [13] J. Hightower and G. Borriello, "Location Systems for Ubiquitous Computing," *IEEE Computer*, vol. 34, no. 8, pp. 57–66, 2001.
- [14] D. Puccinelli and M. Haenggi, "Multipath Fading in Wireless Sensor Networks: Measurements and Interpretation," in *Proceedings of the 2006 International Conference on Communications and Mobile Computing (IWCMC)*. Vancouver, British Columbia, Canada: ACM Press, July 2006, pp. 1039–1044.
- [15] K. Pahlavan and A. H. Levesque, *Wireless Information Networks*. New York: Wiley-Interscience, 1995.